Article

Phytochemicals with Chemopreventive Activity Obtained from the Thai Medicinal Plant *Mammea siamensis* (Miq.) T. Anders.: Isolation and Structure Determination of New Prenylcoumarins with Inhibitory Activity against Aromatase

Fenglin Luo [1], Yoshiaki Manse [1], Saowanee Chaipech [1,2], Yutana Pongpiriyadacha [3], Osamu Muraoka [1] and Toshio Morikawa [1,*]

[1] Pharmaceutical Research and Technology Institute, Kindai University, 3-4-1 Kowakae, Higashi-osaka 577-8502, Osaka, Japan
[2] Faculty of Agro-Industry, Rajamangala University of Technology Srivijaya, Thungyai, Nakhon Si Thammarat 80240, Thailand
[3] Faculty of Science and Technology, Rajamangala University of Technology Srivijaya, Thungyai, Nakhon Si Thammarat 80240, Thailand
[*] Correspondence: morikawa@kindai.ac.jp; Tel.: +81-6-4307-4306; Fax: +81-6-6729-3577

Abstract: With the aim of searching for phytochemicals with aromatase inhibitory activity, five new prenylcoumarins, mammeasins K (**1**), L (**2**), M (**3**), N (**4**), and O (**5**), were isolated from the methanolic extract of *Mammea siamensis* (Miq.) T. Anders. flowers (fam. Calophyllaceae), originating in Thailand. The stereostructures of **1–5** were elucidated based on their spectroscopic properties. Among the new compounds, **1** (IC_{50} = 7.6 μM) and **5** (9.1 μM) possessed relatively strong inhibitory activity against aromatase, which is a target of drugs already used in clinical practice for the treatment and prevention of estrogen-dependent breast cancer. The analysis through Lineweaver–Burk plots showed that they competitively inhibit aromatase (**1**, Ki = 3.4 μM and **5**, 2.3 μM). Additionally, the most potent coumarin constituent, mammea B/AB cyclo D (**31**, Ki = 0.84 μM), had a competitive inhibitory activity equivalent to that of aminoglutethimide (0.84 μM), an aromatase inhibitor used in therapeutics.

Keywords: *Mammea siamensis*; mammeasin; aromatase inhibitor; prenylcoumarin; Calophyllaceae; Lineweaver–Burk analysis

1. Introduction

Coumarins are naturally occurring heterocyclic compounds characterized by 2*H*-chromen-2-one, benzo-α-pyrone, or 2*H*-1-benzopyrane-2-one structures with a common C6-C3 skeleton. In other words, the coumarin skeleton is formed by a benzene ring fused with α-pyrone (lactone ring). This framework is rich in electrons and has good charge-transport properties. Coumarin biosynthesis occurs through the shikimate pathway, which leads to phenylalanine formation and amino acid, which is further converted to cinnamic acid. Numerous enzymes are involved in the biosynthesis of different types of coumarins, such as prenylcoumarins, linear and angular furanocoumarins, pyranocoumarins, methylendioxy-coumarins, hydroxylated and methoxylated coumarins, and coumarin glycosides [1–7]. Most coumarin compounds occur as secondary metabolites in green plants, while some are produced by fungi and bacteria and were obtained from natural resources using column chromatography and preparative HPLC. The structure determination of these coumarins were elucidated based on their spectroscopic properties as well as of their chemical evidence. A variety of pharmacological activities have been reported for coumarins and their analogs, including anticoagulant, anticancer, antioxidant, antiviral, antidiabetic, anti-inflammatory, antibacterial, antifungal, antileishmanial, and

antineurodegenerative activities [3,5–13]. Our studies on the bioactive constituents from medicinal plants, such as *Angelica furcijuga* Kitagawa [14–17] and *Mammea siamensis* (Miq.) T. Anders. [18–22], have been indicated in several bio-functional properties of coumarins, including anti-inflammatory [16–18], hepatoprotective [17], aromatase [19,20] and 5α-reductase inhibitory [21], and anti-proliferative activities [22]. We attempted a further separation of the constituents from the flower part of *M. siamensis* (Calophyllaceae family), which is traditionally used in Thailand as a heart tonic, antipyretic, and appetite enhancer. We focused on isolating five new prenylcoumarins named mammeasins K (**1**), L (**2**), M (**3**), N (**4**), and O (**5**), elucidating their stereostructures and investigating their aromatase inhibitory activity.

2. Results and Discussion

2.1. Isolation

The methanolic extract obtained from the dried flowers of *M. siamensis* (25.66% from the dried material) was partitioned using a solution of ethyl acetate (EtOAc)-H_2O (1:1, *v/v*), yielding an EtOAc-soluble fraction (6.84%) and an aqueous phase. The latter was subjected to Diaion HP-20 column chromatography ($H_2O \rightarrow$ MeOH) according to previously reported protocols, which yielded H_2O- and MeOH-eluted fractions (13.50% and 4.22%, respectively). From the EtOAc-soluble fraction, we previously isolated 37 coumarin constituents (**6–42**) using normal-phase silica gel and reversed-phase ODS column chromatographic purification, and finally HPLC [18–22]. In this study, mammeasins K (**1**, 0.0008%), L (**2**, 0.0006%), M (**3**, 0.0021%), N (**4**, 0.0007%), and O (**5**, 0.0015%) were isolated (Figure 1).
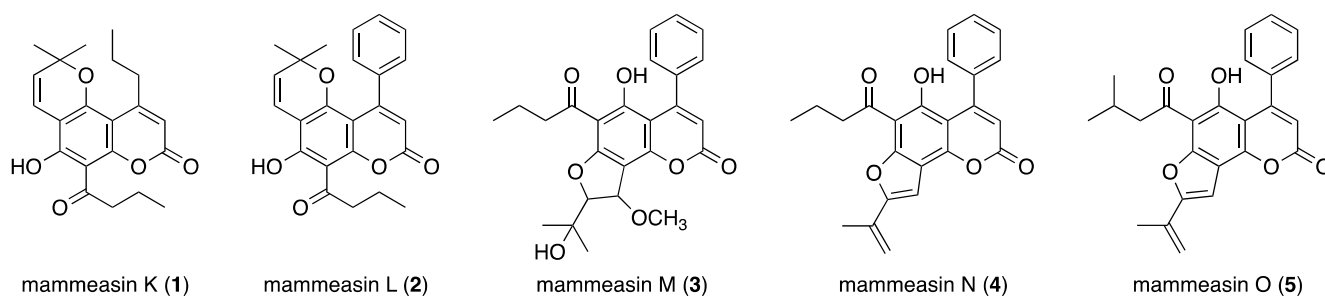
Figure 1. Structures of mammeasins K–O (**1–5**).

2.2. Structure Determination for Mammeasins K (*1*), L (*2*), M (*3*), N (*4*), and O (*5*)

Mammeasin K (**1**) was isolated as pale yellow amorphous solid. The IR spectrum of **1** showed absorption bands at 1748 and 1653 cm^{-1}, assignable to an α,β-unsaturated δ-lactone moiety and a chelated carbonyl group of an aryl keto group, respectively [22–25]. The molecular formula was determined to be $C_{21}H_{24}O_5$ by positive- and negative-ion high-resolution ESI–MS at *m/z* 379.1512 (Calcd for $C_{21}H_{25}O_5Na$, 379.1516) and *m/z* 355.1552 (Calcd for $C_{21}H_{23}O_5$, 355.1540), respectively. The ^{1}H- and ^{13}C-NMR spectra of **1** (Table 1, CDCl$_3$) were assigned with the aid of distortionless enhancement by polarization transfer (DEPT), ^{1}H–^{1}H correlation spectroscopy (COSY), heteronuclear single quantum coherence (HSQC), and heteronuclear multiple bond connectivity (HMBC) experiments (Figure 2). The ^{1}H-NMR spectrum showed signals for four methyls (δ 1.03 (3H, t, *J* = 7.6 Hz, H$_3$-4‴), 1.04 (3H, t, *J* = 7.6 Hz, H$_3$-3′), and 1.53 (6H, s, H$_3$-5″, and H$_3$-6″)), four methylenes (δ 1.66 (2H, qt, *J* = 7.6, 7.6 Hz, H$_2$-2′), 1.78 (2H, qt, *J* = 7.6, 7.3 Hz, H$_2$-3‴), 2.90 (2H, t, *J* = 7.6 Hz, H$_2$-1′), and 3.26 (2H, t, *J* = 7.1 Hz, H$_2$-2‴)), three olefinic protons (δ 5.57 (1H, d, *J* = 10.1 Hz, H-3″), 6.00 (1H, s, H-3), and 6.73 (1H, d, *J* = 10.1 Hz, H-4″)), and a hydrogen-bonded hydroxy proton (δ 14.50 (1H, s, 7-OH)). The ^{1}H- and ^{13}C-NMR spectroscopic properties of **1** were superimposable to those of deacetylmammea E/BC cyclo D (**35**) [18], except for the signal detected owing to the presence of the hydroxy group at the 1′-position of **35**. The ^{1}H–^{1}H COSY experiment on **1** indicated the presence of partial structures shown in bold

lines in Figure 2. In the HMBC experiment, long-range correlations were observed between the following proton and carbon pairs: H-3 and C-2, 4a, 1′; H_2-1′ and C-3, 4, 4a; H-3″ and C-6, 2″; H-4″ and C-5, 7, 2″; H_3-5″ and H_3-6″ and C-2″, 3″; H_2-2‴ and C-1‴; and 7-OH and C-6–8. Thus, the linkage positions of the 2,2-dimethyl-2*H*-pyran and butyryl groups at the coumarin skeleton in **1** were clarified and further confirmed by a comparison of the proton and carbon signals in the ^{1}H- and ^{13}C-NMR spectra of **1** with those of mammea B/AC cyclo D (**32**) [24], which have the opposite linkage of the 2,2-dimethyl-2*H*-pyran and butyryl groups as **1**. Consequently, the structure of **1** was determined.

Table 1. ^{1}H and ^{13}C NMR spectroscopic data (CDCl$_3$) of mammeasins K (**1**) and mammea B/AC cyclo D (**32**).

Position	1 [a]		Position	Mammea B/AC Cyclo D (32) [24] [b]	
	δ_H	δ_C		δ_H	δ_C
2		159.2	2		160.06
3	6.00 (1H, s)	110.5	3	5.93 (1H, s)	110.32
4		158.4	4		159.49
4a		102.7	4a		103.22
5		156.5	5		165.11
6		105.9	6		106.99
7		163.0	7		157.67
8		104.3	8		101.50
8a		157.4	8a		155.09
7-OH	14.50 (1H, s)		5-OH	15.34 (1H, s)	
1′	2.90 (2H, t, 7.6)	39.0	1′	2.92 (2H, dd, 7.5, 7.6)	38.45
2′	1.66 (2H, qt, 7.6, 7.6)	23.3	2′	1.63 (2H, br sext)	22.74
3′	1.04 (3H, t, 7.6)	13.9	3′	0.99 (3H, t, 7.3)	13.98
2″		79.6	1″		207.47
3″	5.57 (1H, d, 10.1)	126.3	2″	3.06 (2H, t, 7.4)	46.88
4″	6.73 (1H, d, 10.1)	115.9	3″	1.72 (2H, sext, 7.4)	18.28
5″	1.53 (3H, s)	28.2	4″	1.00 (3H, t, 7.4)	13.90
6″	1.53 (3H, s)	28.2	2‴		79.65
1‴		206.4	3‴	5.57 (1H, d, 10.0)	126.20
2‴	3.26 (2H, t, 7.1)	46.7	4‴	6.81 (1H, d, 10.0)	115.67
3‴	1.78 (2H, qt, 7.6, 7.1)	18.0	5‴	1.52 (3H, s)	28.69
4‴	1.03 (3H, t, 7.6)	13.8	6‴	1.52 (3H, s)	29.69

Measured by [a] 800 MHz and [b] 400 MHz.
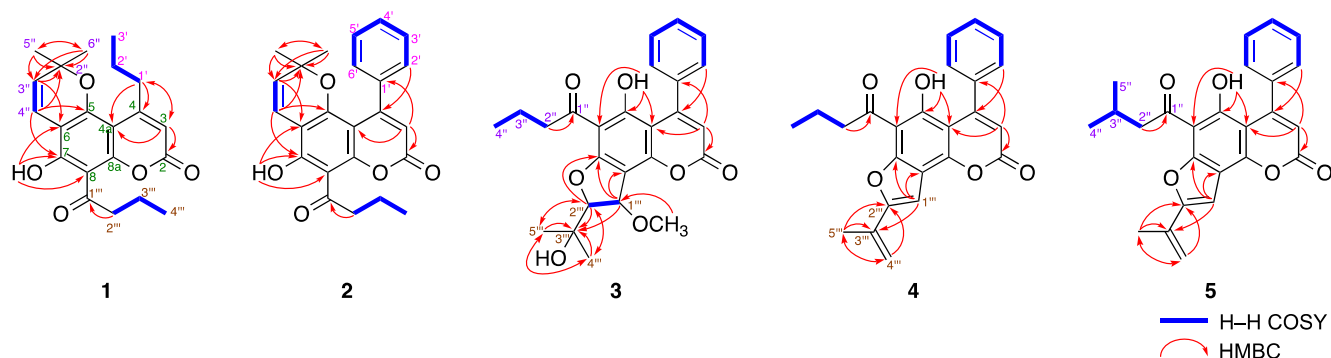
Figure 2. ^{1}H–^{1}H COSY and HMBC correlations of **1–5**.

The molecular formula of mammeasin L (**2**) was determined to be $C_{24}H_{22}O_5$, which showed quasi-molecular ion peaks at *m/z* 413.1353 ([M+Na]$^+$: Calculated for $C_{24}H_{22}O_5Na$, 413.1359) and *m/z* 389.1384 ([M–H]$^−$: Calculated for $C_{24}H_{21}O_5$, 389.1384) using positive- and negative-ion ESI–MS measurements, respectively. The ^{1}H- and ^{13}C-NMR spectra (Table 2, CDCl$_3$) of **2** were similar to those of **1**, except for the signals owing to a mono-substituted benzene ring at the 4-position [δ 7.23 (2H, dd, *J* = 1.6, 7.8 Hz, H-2′ and 6′) and 7.39 (3H, m, H-3′–5′)] instead of a propyl moiety, as seen in **1**. As shown in Figure 2, the connectivity of the quaternary carbons in **2** was elucidated by ^{1}H–^{1}H COSY and HMBC experiments. ^{1}H–^{1}H COSY correlations indicated the presence of the following partial

structures of **2**: linkage of C-2′–C-6′; C-2″–C-4″; and C-2‴–C-4‴ shown in bold line. The HMBC correlations revealed long-range correlations between the following proton and carbon pairs: H-3 (δ 6.01 (1H, s)) and C-2, 4a, 1′; H$_2$-2′, 6′ and C-4; H-3″ (δ 5.39 (1H, d, J = 10.1 Hz)) and C-6, 2″; H-4″ (δ 6.63 (1H, d, J = 10.1 Hz)) and C-5, 7, 2″; H$_3$-5″ and H$_3$-6″ (δ 0.95 (6H, s)) and C-2″, 3″; H$_2$-2‴ (δ 3.31 (2H, t, 7.3)) and C-1‴; and 7-OH (δ 14.50 (1H, s, 7-OH)) and C-6–8. Additionally, different proton and carbon signals owing to the 2,2-dimethyl-2*H*-pyran and butyryl groups of **2** were observed similar with those of mammea A/AC cyclo D (**30**) [24]. Thus, the structure of **2** was established.

Table 2. ^{1}H and ^{13}C NMR spectroscopic data (CDCl$_3$) of mammeasins L (**2**) and mammea A/AC cyclo D (**30**).

Position	2 [a]		Position	Mammea A/AC Cyclo D (30) [24] [b]	
	δ_H	δ_C		δ_H	δ_C
2		158.9	2		159.63
3	6.01 (1H, s)	111.9	3	5.96 (1H, s)	112.66
4		156.0	4		156.38
4a		102.2	4a		102.15
5		156.2	5		164.37
6		105.8	6		106.97
7		163.6	7		158.20
8		104.0	8		101.48
8a		157.0	8a		154.79
7-OH	14.59 (1H, s)		5-OH	14.73 (1H, s)	
1′		140.0	1′		139.21
2′,5′	7.23 (2H, dd, 1.6, 7.8)	127.1	2′,5′	7.29 (2H, m)	127.15
3′,6′	7.39 (2H, m)	127.6	3′,6′	7.38 (2H, m)	127.60
4′	7.39 (1H, m)	127.8	4′	7.38 (1H, m)	128.21
2″		79.0	1″		207.20
3″	5.39 (1H, d, 10.1)	126.8	2″	3.02 (2H, t, 7.3)	46.79
4″	6.63 (1H, d, 10.1)	115.3	3″	1.67 (2H, sext, 7.3)	18.19
5″	0.95 (3H, s)	27.4	4″	0.97 (3H, t, 7.3)	13.07
6″	0.95 (3H, s)	27.4	2‴		79.84
1‴		206.2	3‴	5.60 (1H, d, 10.0)	126.31
2‴	3.31 (2H, t, 7.3)	46.6	4‴	6.86 (1H, d, 10.0)	115.51
3‴	1.82 (2H, qt, 7.6, 7.3)	18.1	5‴	1.55 (3H, s)	28.26
4‴	1.07 (3H, t, 7.6)	13.8	6‴	1.55 (3H, s)	28.26

Measured by [a] 800 MHz and [b] 400 MHz.

Mammeasin M (**3**) was obtained as a pale yellow amorphous solid and its IR spectrum showed absorption bands at 1748 and 1615 cm^{-1}, assignable to an α,β-unsaturated δ-lactone moiety and a chelated carbonyl group of an aryl keto moiety [22–25]. The EI–MS spectrum of **3** showed a molecular ion peak at *m/z* 438.1679 (M$^+$) and the molecular formula was determined to be C$_{25}$H$_{26}$O$_7$ (Δ + 0.3 mmu) using high-resolution EI–MS measurements. The ^{1}H-NMR spectra of **3** (Table 3, CDCl$_3$) showed signals indicating the presence of three methyls (δ 0.98 (3H, t, J = 7.5 Hz, H$_3$-4″), 1.35 and 1.39 (3H each, both s, H$_3$-4‴ and 5‴)); two methylenes (δ 1.70 (2H, qt, J = 7.5, 7.2 Hz, H$_2$-3″), 3.00 (2H, t, J = 7.2 Hz, H$_2$-2″)); a methoxymethyl (δ 3.64 (3H, s)); two methine bearing an oxygen function (δ 4.65 and 5.23 (1H each, both d, J = 2.9 Hz, H-2‴ and 1‴)); an olefinic proton (δ 5.98 (1H, s, H-3)); a mono-substituted benzene ring (δ 7.30 (2H, dd, J = 1.7, 8.1 Hz, H-2′ and 6′), 7.34 (1H, m, H-4′), 7.40 (2H, dd, J = 7.2, 8.1 Hz, H-3′ and 5′)), and a hydrogen-bonded hydroxy proton (δ 14.65 (1H, s, 5-OH)). The planar structure of **3** was constructed using ^{1}H-^{1}H COSY and HMBC experiments. Thus, ^{1}H-^{1}H COSY of **3** indicated the presence of partial structures, as shown in bold lines in Figure 2. In the HMBC experiment, long-range correlations were observed between the following proton and carbon pairs: H-3 and C-2, 4a, 1′; H$_2$-2′, 6′ and C-4; H-2″ and C-1″; H-1‴ and C-7, 8, 3‴; H-2‴ and C-7, 3‴–5‴; H$_3$-4‴ and C-2‴, 3‴,5‴; H$_3$-5‴ and C-2‴–4‴; 5-OH and C-4a, 5, 6; and 1‴-OCH$_3$ and C-1‴. Next, the stereochemistry of the 2-(3-methoxy-2,3-dihydrofuran-2-yl)propan-2-ol moiety in **3** was clarified by comparing the ^{1}H-^{1}H coupling constant between H-1‴ and H-2‴ and by nuclear Overhauser effect (NOE) difference spectrometry. As shown in Figure 3,

the coupling constant in the ^{1}H-NMR spectrum of **3** showed $^3J_{1''',2'''} = 2.9$ Hz, similar to that of the related compound mammea A/AA methoxycyclo F (**3a**, $J = 3.0$ Hz) [26,27]. Furthermore, a NOE correlation was observed between H-2''' and 1'''-OCH$_3$ (Figure 3), so that the relative stereochemistry of H-1''' and H-2''' was determined to be *trans*. Based on these findings, the structure of **3** was determined.

Table 3. ^{1}H and ^{13}C NMR spectroscopic data (500 mHz, CDCl$_3$) of mammeasin M (**3**) and mammea A/AA methoxycyclo F (**3a**).

Position	3		Mammea A/AA Methoxycyclo F (3a) [26]	
	δ_H	δ_C	δ_H	δ_C
2		159.2		159.8
3	5.98 (1H, s)	112.6	5.99 (1H, s)	112.5
4		156.5		156.5
4a		102.8		102.8
5		166.3		166.5
6		103.0		103.3
7		165.2		164.4
8		106.0		105.9
8a		156.5		156.8
5-OH	14.65 (1H, s)		14.75 (1H, s)	
1'		139.0		139.0
2',5'	7.30 (2H, dd, 1.7, 8.1)	127.2	7.31 (2H, m)	127.2
3',6'	7.40 (2H, dd, 7.2, 8.1)	127.7	7.40 (2H, m)	127.7
4'	7.34 (1H, m)	128.3	7.40 (1H, m)	128.3
1''		205.3		205.1
2''	3.00 (2H, t, 7.2)	45.2	2.81 (1H, dd, 7.0, 15.0) 3.00 (1H, dd, 7.0, 15.0)	52.0
3''	1.70 (2H, qt, 7.5, 7.2)	17.8	2.21 (1H, m)	25.0
4''	0.98 (3H, t, 7.2)	13.8	0.96 (3H, d, 7.0)	22.6
5''			0.96 (3H, d, 7.0)	22.6
1'''	5.23 (1H, d, 2.9)	78.7	5.23 (1H, d, 3.0)	78.6
2'''	4.65 (1H, d, 2.9)	97.8	4.65 (1H, d, 3.0)	97.7
3'''		71.2		71.2
4'''	1.35 (3H, s)	25.6	1.35 (3H, s)	25.5
5'''	1.39 (3H, s)	25.9	1.39 (3H, s)	25.9
1'''-OCH$_3$	3.64 (3H, s)	57.7	3.64 (3H, s)	57.7
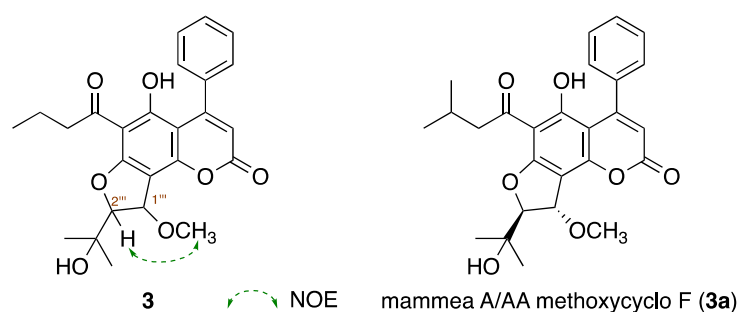
Figure 3. Coupling constant $^3J_{1''',2'''}$ value and difference NOE correlation of **3**. Reported value (CDCl$_3$) of mammea A/AA methoxycyclo F (**3a**).

Using high-resolution negative-ion ESI–MS analyses, the molecular formulae of mammeasins N (**4**) and O (**5**) were determined to be C$_{24}$H$_{20}$O$_5$ and C$_{25}$H$_{22}$O$_5$, respectively. The ^{1}H- and ^{13}C-NMR spectra (Table 4) of **4** showed signals assignable to a butane-1-one moiety (δ 1.06 (3H, t, $J = 7.4$ Hz, H$_3$-4''), 3.16 (2H, t, $J = 7.4$ Hz, H$_2$-2''), 1.81 (2H, qt, $J = 7.4$, 7.4 Hz, H$_2$-3''); δ_C 13.8 (C-4''), 17.7 (C-3''), 45.1 (C-2''), 204.5 (C-1'')) together with a methyl (δ 2.16 (3H, s, H$_3$-4''')), an *exo*-methylene (δ 5.52, 5.71 (1H each, both s, H$_2$-5''')), two olefins (δ 6.14 (1H, s, H-3), 6.98 (1H, s, H-1''')), a mono-substituted benzene ring (δ 7.35 (2H, dd, $J = 1.7$, 7.7 Hz, H-2' and 6'), 7.34 (3H, m, H-3'–5')), and a hydrogen-bonded hydroxy proton (δ 14.58 (1H, s, 5-OH)). The connectivities of the quaternary carbons in **4** and **5** were characterized using ^{1}H-^{1}H COSY and HMBC experiments, which showed long-range

correlations, as shown in Figure 2. Furthermore, the proton and carbon signals for 2-(prop-1-en-2-yl)furan moiety in **4** were superimposable with those of the corresponding furanocoumarin oroselone (**4a**), as shown in Figure 4 [28]. The proton and carbon signals in the ^{1}H- and 13C-NMR spectra (Table 4) of **5** were quite similar to those of **4**, except for the signals arising from a 3-methylbutane-1-one moiety (δ 1.03 (6H, d, *J* = 6.8 Hz, H$_3$-4″ and 5″), 2.32 (1H, m, H-3″), 3.16 (2H, d, *J* = 6.9 Hz, H$_2$-2″); δ_C 22.7 (C-4″ and 5″), 25.0 (C-3″), 51.8 (C-2″), 204.3 (C-1″)). Consequently, the structures of **4** and **5** were determined.

Table 4. ^{1}H and ^{13}C NMR spectroscopic data (CDCl$_3$) of mammeasins M (**3**) and N (**4**) and oroselone (**4a**).

Position	4 [a]		5 [b]		Oroselone (4a) [28]	
	δ_H	δ_C	δ_H	δ_C	δ_H	δ_C
2		159.3		159.3		160.62
3	6.14 (1H, s)	114.2	6.14 (1H, s)	114.2	6.36 (1H, d, 9.6)	113.88
4		156.7		156.5	7.77 (1H, d, 9.6)	144.32
4a		103.3		103.6		113.40
5		162.8		163.0	7.30 (1H, d, 8.5)	123.79
6		104.6		104.7	7.34 (1H, d, 8.5)	108.21
7		155.7		156.4		156.90
8		111.2		111.3		118.29
8a		153.1		153.1		148.08
5-OH	14.58 (s)		14.58 (s)			
1′		138.9		138.9		
2′,5′	7.35 (2H, dd, 1.7, 7.7)	127.2	7.36 (2H, dd, 1.7, 7.8)	127.2		
3′,6′	7.43 (2H, m)	127.7	7.43 (2H, m)	127.7		
4′	7.43 (1H, m)	128.4	7.43 (1H, m)	128.4		
1″		204.5		204.3		
2″	3.26 (2H, t, 7.4)	45.1	3.16 (2H, d, 6.9)	51.8		
3″	1.81 (2H, qt, 7.4, 7.4)	17.7	2.32 (1H, m)	25.0		
4″	1.06 (3H, t, 7.4)	13.8	1.03 (3H, d, 6.8)	22.7		
5″			1.03 (3H, d, 6.8)	22.7		
1‴	6.98 (1H, s)	100.2	6.98 (1H, s)	100.3	6.96 (1H, s)	99.59
2‴		156.5		156.7		157.94
3‴		132.0		132.0		132.18
4‴	5.25 (1H, br s)5.71 (1H, br s)	113.4	5.25 (1H, br s)5.71 (1H, br s)	113.3	5.24 (1H, s) 5.82 (1H, s)	118.29
5‴	2.16 (3H, s)	19.1	2.16 (3H, s)	19.1	2.13 (3H, s)	19.06

Measured by [a] 800 MHz or [b] 500 MHz.
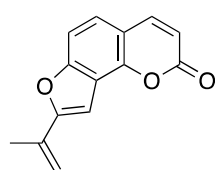
oroselone (**4a**)

Figure 4. Structure of oroselone (**4a**).

2.3. Inhibitory Activity against Aromatase

In a recent exploratory study on the bioactive constituents of *M. siamansis*, several coumarins exhibited antiproliferative and apoptotic effects in several human cancer cell lines. Furthermore, their mechanisms of action have also been characterized [29–33]. We have also reported that these coumarin constituents exhibit antiproliferative and apoptotic effects against human digestive tract carcinoma cell lines and human breast cancer MCF-7 [22]. Breast cancer is one of the malignant carcinomas associated with the highest morbidity and mortality in women [34,35]. The presence of high estrogen concentrations in breast tissue increases the risk of developing breast cancer. Estrogen and estrogen receptors play an important role in the development and progression of hormone-dependent breast cancer [36]. Aromatase is a key enzyme in estrogen biosynthesis, as it catalyzes the conversion of androgens (testosterone and androstenediol) to estrogens (estradiol and

estrone). Since intra-tumoral aromatase is the source of estrogen production in breast cancer tissues, aromatase inhibitors have been widely used in clinical practice as chemotherapeutic agents against hormone-dependent breast cancer [37]. Based on their chemical structures, aromatase inhibitors are classified into two categories: steroidal and non-steroidal [38]. The structures of steroidal aromatase inhibitors closely resemble those of the substrates of aromatase enzymes, such as testosterone and androstenediol. Exemestane, a clinically used steroidal aromatase inhibitor, is metabolized to an intermediate, which attaches irreversibly to the active site of the enzyme, thereby blocking its activity. These inhibitors are known as "suicide inhibitors" [37]. On the other hand, non-steroidal aromatase inhibitors (e.g., aminoglutethimide, anastrozole, and letrozole, etc.) are generally reversible, and the inhibition of estrogen synthesis is dependent on the continuous presence of the drug [39]. Owing to the development of resistance to aromatase inhibitors and their side effects, the need for improved aromatase inhibitors remains [40,41]. Therefore, new non-steroidal natural products with aromatase inhibitory activity are being investigated [36,42–45]. During our studies of characterization of the Thai medicinal plant *M. siamensis*, we found that the methanolic extract and several isolated coumarin constituents exhibited inhibitory activity against aromatase [19]. Continuing the chemical study on *M. siamemsis*, we have so far isolated 42 coumarin constituents, as summarized in Figure 5.

Fifteen such coumarin constituents, including mammeasins K (**1**, IC_{50} = 7.6 μM) and O (**5**, 9.1 μM); kayaessamin I (**23**, 9.3 μM); mammea A/AA cyclo F (**39**, 9.2μM); mammeasins A (**6**, 8.7 μM), B (**7**, 4.1 μM), C (**8**, 2.7 μM), and D (**9**, 3.6 μM); surangins B (**16**, 9.8 μM), C (**17**, 8.8 μM), and D (**18**, 9.8 μM); mammea A/AA (**24**, 6.9 μM), A/AB (**25**, 8.6 μM), A/AA cyclo D (**28**, 7.2 μM); and B/AB cyclo D (**3**.1 μM) [19], show relatively strong aromatase enzymatic inhibitory activities (IC_{50} ranging from 2.7–9.9 μM), comparable to the activity of the clinically used nonsteroidal aromatase inhibitor aminoglutethimide (2.0 μM), as shown in Table 5.

We analyzed inhibition kinetics using Lineweaver–Burk plots to determine the mode of inhibition of coumarins that showed strong inhibitory activities against human aromatase. In the assay system, we fixed the enzyme concentration, changed the substrate concentration, and obtained the kinetic parameters of the enzyme-catalyzed reaction using Lineweaver–Burk double reciprocal plot 1/[V] vs. 1/[S]. The inhibition constant K_i indicates the potency of an inhibitor and equals the concentration required to produce half-maximal inhibition [46]. The K_i value was obtained from the intersection of the secondary plot with the *x*-axis (apparent K_m/V_{max} vs. inhibitor). Thus, the first-generation aromatase inhibitor aminoglutethimide showed a competitive inhibition of aromatase characterized by a K_i value of 0.84 μM, as shown in Table 6 and Figure 6, which is consistent with the results of a previous report [47]. Among the active coumarin constituents from *M. siamensis*, mammeasins K (**1**, *K*i value = 3.4 μM), N (**4**, 2.6 μM), and O (**5**, 2.3 μM); as well as B (**7**, 1.3 μM) and C (**8**, 2.8 μM); surangins B (**16**, 1.3 μM) and C (**17**, 2.6 μM); and mammeas A/AA cyclo D (**28**, 1.2 μM), B/AB cyclo D (**31**, 0.84 μM), and E/BC cyclo D (**33**, 2.3 μM), show relatively potent competitive inhibition. The most potent compound, **31**, exhibited almost the same binding affinity as aminoglutethimide.

mammeasin A (**6**)   mammeasin B (**7**)   mammeasin C (**8**)   mammeasin D (**9**)

mammeasin E (**10**)   mammeasin F (**11**)   mammeasin G (**12**)   mammeasin H (**13**)   mammeasin I (**14**)   mammeasin J (**15**)

surangin B (**16**)   surangin C (**17**)   surangin D (**18**)   kayeassamin A (**19**)

kayeassamin E (**20**)   kayeassamin F (**21**)   kayeassamin G (**22**)   kayeassamin I (**23**)   mammea A/AA (**24**)   mammea A/AB (**25**)

mammea A/AC (**26**)   mammea A/AD (**27**)   mammea A/AA cyclo D (**28**)   mammea A/AB cyclo D (**29**)   mammea A/AC cyclo D (**30**)

mammea B/AB cyclo D (**31**)   mammea B/AC cyclo D (**32**)   mammea E/BC cyclo D (**33**)   mammea E/BD cyclo D (**34**)   deacetylmammea E/BC cyclo D (**35**)

mammea E/BA (**36**)   mammea E/BB (**37**)   mammea E/BC (**38**)   mammea A/AA cyclo F (**39**)   mammea A/AC cyclo F (**40**)

deacetylmammea E/AA cyclo D (**41**)   deacetylmammea E/BB cyclo D (**42**)

Figure 5. Coumarin constituents (**6–42**) from the flowers of *M. siamensis*.

Table 5. IC_{50} values of coumarin constituents (**1–11**, **16**, **17**, **23–25**, **28**, **31**, **34**, **38**, and **39**) from the flowers of *M. siamensis* against human recombinant aromatase.

Treatment	IC_{50} (μM)	Treatment	IC_{50} (μM)
Mammeasin K (**1**)	7.6	Kayaessamin G (**22**)	27.8 [19]
Mammeasin L (**2**)	20.7	Kayaessamin I (**23**)	9.3
Mammeasin M (**3**)	>100 (43.4) [a]	Mammea A/AA (**24**)	6.9 [19]
Mammeasin N (**4**)	12.0	Mammea A/AB (**25**)	8.6 [19]
Mammeasin O (**5**)	9.1	Mammea A/AC (**26**)	13.7 [19]
Mammeasin A (**6**)	8.7 [19]	Mammea A/AD (**27**)	11.3 [19]
Mammeasin B (**7**)	4.1 [19]	Mammea A/AA cyclo D (**28**)	7.2 [19]
Mammeasin C (**8**)	2.7 [19]	Mammea A/AB cyclo D (**29**)	24.1 [19]
Mammeasin D (**9**)	3.6 [19]	Mammea A/AC cyclo D (**30**)	35.0 [19]
Mammeasin E (**10**)	11.1	Mammea B/AB cyclo D (**31**)	3.1 [19]
Mammeasin F (**11**)	12.4	Mammea B/AC cyclo D (**32**)	24.6 [19]
Mammeasin G (**12**)	21.3	Mammea E/BC cyclo D (**33**)	11.5 [19]
Mammeasin H (**13**)	17.9	Mammea E/BD cyclo D (**34**)	21.1
Mammeasin I (**14**)	21.3	Deacetylammea E/BC cyclo D (**35**)	16.6 [19]
Mammeasin J (**15**)	23.4	Mammea E/BA (**36**)	16.6 [19]
Surangin B (**16**)	9.8 [19]	Mammea E/BB (**37**)	18.6 [19]
Surangin C (**17**)	8.8 [19]	Mammea E/BC (**38**)	23.2
Surangin D (**18**)	9.8 [19]	Mammea A/AA cyclo F (**39**)	9.2
Kayeassamin A (**19**)	10.0	Mammea A/AC cyclo F (**40**)	19.9
Kayeassamin E (**20**)	14.9 [19]	Deacetylammea E/AA cyclo D (**41**)	19.3
Kayeassamin F (**21**)	19.7 [19]	Deacetylammea E/BB cyclo D (**42**)	12.1
		Aminoglutethimide	2.0 [19]

Each value represents the mean ± S.E.M. (*N* = 3). [a] Values in parentheses represent inhibition % at 100 μM.

Table 6. K_i values of coumarin constituents (**1–11**, **16**, **17**, **23–25**, **28**, **31**, **34**, **38**, and **39**) from the flowers of *M. siamensis* against human recombinant aromatase.

Treatment	K_i (μM)	Treatment	K_i (μM)
Mammeasin K (**1**)	3.4	Surangin C (**17**)	2.6
Mammeasin N (**4**)	2.6	Kayaessamin I (**23**)	14.7
Mammeasin O (**5**)	2.3	Mammea A/AA (**24**)	13.7
Mammeasin A (**6**)	5.1	Mammea A/AB (**25**)	8.1
Mammeasin B (**7**)	1.3	Mammea A/AA cyclo D (**28**)	1.2
Mammeasin C (**8**)	2.8	Mammea B/AB cyclo D (**31**)	0.84
Mammeasin D (**9**)	4.3	Mammea E/BC cyclo D (**33**)	2.3
Mammeasin E (**10**)	7.1	Mammea E/BC (**38**)	11.3
Mammeasin F (**11**)	12.3	Mammea A/AA cyclo F (**39**)	4.3
Surangin B (**16**)	1.3		
		Aminoglutethimide	0.84

Each value represents the mean ± S.E.M. (*N* = 3).
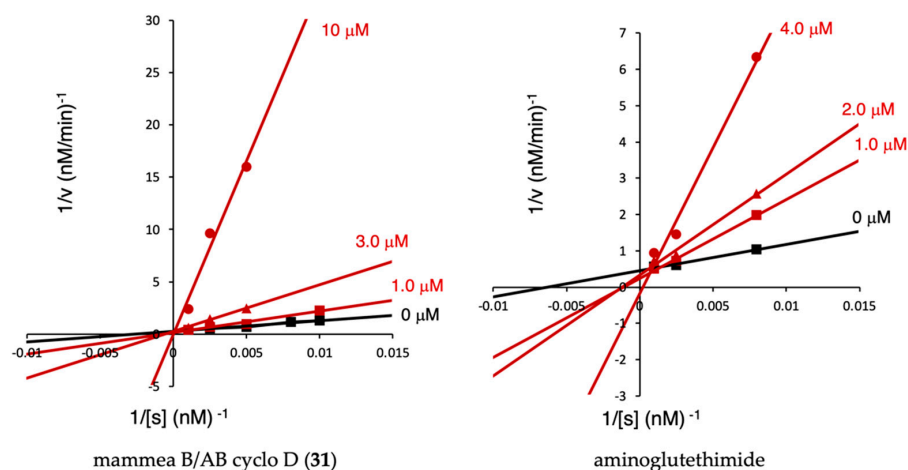
Figure 6. Lineweaver-Burk plots of the inhibition of human recombinant aromatase activities by mammea B/AB cyclo D (**31**) and aminoglutethimode.

3. Materials and Methods

3.1. General

The following instruments were used to obtain spectroscopic data: specific rotation, JASCO P-2200 polarimeter (JASCO Corporation, Tokyo, Japan, *l* = 5 cm); UV spectra, Shimadzu UV-1600 spectrometer; IR spectra, IRAffinity-1 spectrophotometer (Shimadzu Co., Kyoto, Japan); ^{1}H NMR spectra, JNM-ECA800 (800 MHz), JNM-LA500 (500 MHz), JNM-ECS400 (400 MHz), and JNM-AL400 (400 MHz) spectrometers; and ^{13}C NMR spectra, JNM-ECA800 (200 MHz), JNM-LA500 (125 MHz), JNM-ECA400 (100 MHz), and JNM-AL400 (100 MHz) spectrometers (JEOL Ltd., Tokyo, Japan). Determinations were made using samples dissolved in deuterated chloroform ($CDCl_3$) at room temperature with tetramethylsilane as an internal standard; EI–MS and high-resolution EI–MS, JMS–GCMATE mass spectrometer (JEOL Ltd., Tokyo, Japan); ESI–MS and HRESI–MS, Exactive^{TM} Plus Orbitrap mass spectrometer (Thermo Fisher Scientific Inc., Waltham, MA, USA); HPLC detector, SPD-10A*vp* UV–VIS detector; HPLC columns, Cosmosil 5C$_{18}$-MS-II (Nacalai Tesque, Inc., Kyoto, Japan). Columns of 4.6 mm i.d. × 250 mm and 20 mm i.d. × 250 mm were used for analytical and preparative purposes, respectively.

The following experimental chromatographic materials were used for column chromatography (CC): highly porous synthetic resin, Diaion HP-20 (Mitsubishi Chemical Co., Tokyo, Japan); normal-phase silica gel CC, silica gel 60 N (Kanto Chemical Co., Ltd., Tokyo, Japan; 63–210 mesh, spherical, neutral); reversed-phase ODS CC, Chromatorex ODS DM1020T (Fuji Silysia Chemical, Ltd., Aichi, Japan; 100–200 mesh); TLC, pre-coated TLC plates with silica gel 60F$_{254}$ (Merck, Darmstadt, Germany, 0.25 mm) (normal-phase) and silica gel RP-18 WF$_{254S}$ (Merck, 0.25 mm) (reversed-phase); reversed-phase HPTLC, pre-coated TLC plates with silica gel RP-18 WF$_{254S}$ (Merck, 0.25 mm). Detection was performed by spraying with 1% Ce(SO$_4$)$_2$–10% aqueous H$_2$SO$_4$, followed by heating.

3.2. Plant Material

M. siamensis flowers were collected from Nakhonsithammarat Province, Thailand, in September 2006, as described previously [18,19,21,22]. Plant material was identified by one of the authors (Y.P.). A voucher specimen (2006.09. Raj-04) was deposited in our laboratory.

3.3. Extraction and Isolation

The methanolic extract (25.66% dried material) obtained from the dried flowers of *M. siamensis* (1.8 kg) was partitioned using a solution of EtOAc-H$_2$O (1:1, *v/v*) to yield an EtOAc-soluble fraction (6.84%) and an aqueous phase. The EtOAc-soluble fraction (89.45 g) was subjected to normal-phase silica gel column cromatography (3.0 kg, *n*-hexane-EtOAc (10:1 → 7:1 → 5:1, *v/v*) → EtOAc → MeOH) to produce 11 fractions (Fr. 1 (3.05 g), Fr. 2 (2.86 g), Fr. 3 (11.71 g), Fr. 4 (1.62 g), Fr. 5 (4.15 g), Fr. 6 (6.29 g), Fr. 7 (2.21 g), Fr. 8 (2.94 g), Fr. 9 (10.23 g), Fr. 10 (11.17 g), and Fr. 11 (21.35 g)), as previously reported [18]. Fraction 2 (2.86 g) was subjected to reversed-phase silica gel CC (74 g, MeOH–H$_2$O (70:30 → 90:10, *v/v*) → MeOH → acetone) to yield nine fractions (Fr. 2-1 (21.0 mg), Fr. 2-2 (26.2 mg), Fr. 2-3 (114.1 mg), Fr. 2-4 (425.0 mg), Fr. 2-5 (199.3 mg), Fr. 2-6 (79.6 mg), Fr. 2-7 (94.8 mg), Fr. 2-8 (1211.4 mg), and Fr. 2-9 (328.8 mg)), as described previously [22]. Fraction 2-4 (425.0 mg) was purified by HPLC (Cosmosil 5C$_{18}$-MS-II, MeOH–1% aqueous AcOH (90:10, *v/v*) and CH$_3$CN–1% aqueous AcOH (75:25, *v/v*)) to give mammeasins K (**1**, 10.6 mg, 0.0008%) and L (**2**, 8.2 mg, 0.0006%) together with mammeasins G (**12**, 32.7 mg, 0.0025%), H (**13**, 12.1 mg, 0.0009%), and I (**14**, 10.5 mg, 0.0008%) [22]. Fraction 5 (4.15 g) was subjected to reversed-phase silica gel CC (120 g, MeOH–H$_2$O (80:20 → 85:15, *v/v*) → MeOH → acetone) to obtain six fractions (Fr. 5-1 (115.7 mg), Fr. 5-2 (2789.8 mg), Fr. 5-3 (515.4 mg), Fr. 5-4 (430.0 mg), Fr. 5-5 (119.2 mg), and Fr. 5-6 (1110.0 mg)), as previously reported [21]. Fraction 5-2 (517.0 mg) was purified by HPLC (Cosmosil 5C$_{18}$-MS-II, MeOH–1% aqueous AcOH (85:15, *v/v*)) to give mammeasins M (**3**, 5.0 mg, 0.0021%) and O (**5**, 3.7 mg, 0.0015%) together with mammeas A/AA (**24**, 101.2 mg, 0.0418%), A/AC (**26**, 112.9 mg, 0.0466%), A/AA cyclo D (**28**, 3.7 mg, 0.0015%), E/BC cyclo D (**33**, 14.0 mg, 0.0058%), E/BD cyclo D (**34**,

1.8 mg, 0.0007%), and A/AC cyclo F (**40**, 4.6 mg, 0.0019%) [18,19,21]. Fraction 6 (6.29 g) was subjected to reversed-phase silica gel CC (200 g, MeOH–H_2O (80:20 → 90:10 → 95:5, *v/v*) → MeOH → acetone) and 10 fractions were obtained (Fr. 6-1 (44.7 mg), Fr. 6-2 (157.2 mg), Fr. 6-3 (928.8 mg), Fr. 6-4 (3117.0 mg), Fr. 6-5 (128.8 mg), Fr. 6-6 (487.1 mg), Fr. 6-7 (230.8 mg), Fr. 6-8 (280.5 mg), Fr. 6-9 (102.9 mg), and Fr. 6-10 (96.5 mg)), as previously reported [18]. Fraction 6-3 (514.6 mg) was purified by HPLC (Cosmosil 5C18-MS-II, MeOH−1% aqueous AcOH (80:20, *v/v*)) to give mammeasin N (**4**, 5.1 mg, 0.0007%) together with mammeas A/AC (**26**, 35.6 mg, 0.0049%), A/AD (**27**, 15.8 mg, 0.0022%), E/BA (**36**, 32.7 mg, 0.0045%), and E/BB (**37**, 140.1 mg, 0.0190%).

3.3.1. Mammeasin K (**1**)

Pale yellow amorphous solid; high-resolution positive-ion ESI–MS *m/z* 379.1512 (Calculated for $C_{21}H_{25}O_5Na$, 379.1516), negative-ion ESI–MS *m/z* 355.1552 (Calculated for $C_{21}H_{23}O_5$, 355.1540); UV [MeOH, nm (log ε)]: 305 (4.39), 270 (4.46), 219 (4.14); IR (film): 1748, 1734, 1653, 1609, 1558, 1506, 1456, 1387, 1194, 1150, 1125 cm^{-1}; ^{1}H-NMR (800 MHz, $CDCl_3$) δ: see Table 1 and Figure S1; ^{13}C-NMR data (200 MHz, $CDCl_3$) δ_C: see Table 1 and Figure S2; 2D-NMR spectra: see Figures S3–S5; positive-ion ESI–MS *m/z* 379 [M+Na]$^+$; negative-ion ESI–MS *m/z* 355 [M-H]$^-$.

3.3.2. Mammeasin L (**2**)

Pale yellow amorphous solid; high-resolution positive-ion ESI–MS *m/z* 413.1353 (Calculated for $C_{24}H_{22}O_5Na$, 413.1359), negative-ion ESI–MS *m/z* 389.1384 (Calculated for $C_{24}H_{21}O_5$, 389.1384); UV (MeOH, nm (log ε)): 263 (4.41), 309 (4.35); IR (film): 1748, 1734, 1683, 1653, 1610, 1558, 1506, 1456, 1387, 1190, 1153, 1138 cm^{-1}; ^{1}H-NMR (800 MHz, $CDCl_3$) δ: see Table 2 and Figure S6; ^{13}C-NMR data (200 MHz, $CDCl_3$) δ_C: see Table 2 and Figure S7; 2D-NMR spectra: see Figures S8–S10; positive-ion ESI–MS *m/z* 413 [M+Na]$^+$; negative-ion ESI–MS *m/z* 389 [M-H]$^-$.

3.3.3. Mammeasin M (**3**)

Pale yellow amorphous solid; $[\alpha]_D^{23}$ 0 (*c* 0.15, $CHCl_3$); high-resolution EI–MS: Calculated for $C_{25}H_{26}O_7$ (M$^+$): 438.1679. Found: 438.1676; UV (MeOH, nm (log ε)): 281 (4.35); IR (film): 3450, 1748, 1717, 1615, 1558, 1456, 1381, 1235, 1190, 1154 cm^{-1}; ^{1}H-NMR (500 MHz, $CDCl_3$) δ: see Table 3 and Figure S11; ^{13}C-NMR data (125 MHz, $CDCl_3$) δ_C: see Table 3 and Figure S12; 2D-NMR spectra: see Figures S13–S16; EI–MS *m/z* (%): 438 (M$^+$, 16), 309 (100).

3.3.4. Mammeasin N (**4**)

Pale yellow amorphous solid; high-resolution negative-ion ESI–MS *m/z* 387.1238 (Calculated for $C_{24}H_{19}O_5$, 387.1227); UV (MeOH, nm (log ε)): 287 (4.25); IR (film): 1748, 1609, 1559, 1458, 1373, 1230, 1150, 1126 cm^{-1}; ^{1}H-NMR (800 MHz, $CDCl_3$) δ: see Table 4 Figure S17; ^{13}C-NMR data (200 MHz, $CDCl_3$) δ_C: see Table 4 and Figure S18; 2D-NMR spectra: see Figures S19–S21; negative-ion ESI–MS *m/z* 387 [M-H]$^-$.

3.3.5. Mammeasin O (**5**)

Pale yellow amorphous solid; high-resolution negative-ion ESI–MS *m/z* 401.1393 (Calcd for $C_{25}H_{21}O_5$, 401.1394); UV (MeOH, nm (log ε)): 287 (4.26); IR (film): 1748, 1614, 1460, 1392, 1262, 1217, 1156, 1127 cm^{-1}; ^{1}H-NMR (500 MHz, $CDCl_3$) δ: see Table 4 and Figure S22; ^{13}C-NMR data (125 MHz, $CDCl_3$) δ_C: see Table 4 and Figure S23; 2D-NMR spectra: see Figures S24–S26; negative-ion ESI–MS *m/z* 401 [M-H]$^-$.

3.4. Assay for Aromatase Inhibitory Activity

3.4.1. Reagents

Dibenzylfluorescein (DBF) and human CYP19 + P450 reductase SUPERSOMES (human recombinant aromatase) were purchased from BD Biosciences (Heidelberg, Germany) and testosterone from Tokyo Chemical Industry Co., Ltd. (Tokyo, Japan). The other

chemicals used in this study were purchased from Wako Pure Chemical Industries, Co., Ltd. (Osaka, Japan).

3.4.2. Inhibitory Effects against Human Recombinant Aromatase

The experiments were performed according to a previously described method [18]. Briefly, a test sample was dissolved in dimethyl sulfoxide (DMSO), and the solution was diluted with potassium phosphate buffer (50 mM, pH 7.4) containing $MgCl_2$ (0.5 mM) to obtain the test sample solution (concentration of DMSO: 2%). An enzyme/substrate solution in the buffer (20 μL, 1.6 μM DBF, 8 nM human recombinant aromatase) and the test sample solution (20 μL) were mixed in a 96-well half-area black microplate (Greiner Bio-One, Frickenhausen, Germany) at 37 °C for 10 min. The enzymatic reaction was initiated by adding NADPH solution (40 μL, 500 μM) at 37 °C for 30 min. After 30 min of incubation, NaOH (30 μL, 2 mM) was added, and the reaction mixture was incubated at 37 °C for 2 h to induce fluorescent signals (final DMSO concentration, 0.5%; aromatase, 2 nM; and NADPH, 250 μM). Fluorescence was measured using a fluorescence microplate reader (SH-9000, CORONA ELECTRIC Co., Ltd., Ibaraki, Japan) at an excitation wavelength of 435 nm and emission wavelength of 535 nm. Experiments were performed in triplicate, and the IC_{50} values were determined graphically. The aromatase inhibitor, aminoglutethimide, was used as the reference compound.

3.4.3. Kinetic Analysis of Inhibitory Activity against Human Recombinant Aromatase Using Lineweaver-Burk Plots

Experiments were performed using a previously described protocol [18], modified by using various concentrations of testosterone (0.4–4 μM) as substrates instead of DBF and the plate was heated at 37 °C for 15 min. After the reaction, the enzyme was inactivated by heating in a boiling water bath for 2 min. An estradiol EIA kit (Oxford Biomedical Research, Inc., Oxford, MI, USA) was used to develop an estradiol standard curve to determine the concentration of estradiol produced and to correlate the concentration of estradiol with the reaction velocity. The mode of inhibition was analyzed using the Lineweaver–Burk plot of the inverse of the reaction velocity of estradiol plotted on the vertical axis and the inverse of the final concentration of the substrate on the horizontal axis, with and without the test substance (Figure S27).

3.4.4. Statistics

Values are expressed as mean ± standard mean error (S.E.M.). One-way analysis of variance (ANOVA), followed by Dunnett's test, was used for statistical analysis. Probability (*p*) values of less than 0.05 were considered significant.

4. Conclusions

Five new prenylcoumarins, mammeasins K–O (**1–5**), were isolated from the methanolic extract of the flowers of *M. siamensis*, a plant originating from Thailand. The stereostructures of **1–5** were elucidated based on their spectroscopic properties. Fifteen coumarin constituents, including **1** (IC_{50} = 7.6 μM) and **5** (9.1 μM), kayaessamin I (**23**, 9.3 μM), and mammea A/AA cyclo F (**39**, 9.2 μM), showed relatively strong aromatase enzymatic inhibitory activities, comparable to the activity of a clinically used nonsteroidal aromatase inhibitor aminoglutethimide (2.0 μM). On the basis of *Ki* values, **1** (*Ki* value = 3.4 μM), **4** (2.6 μM), **5** (2.3 μM); mammeasins B (**7**, 1.3 μM) and C (**8**, 2.8 μM); surangins B (**16**, 1.3 μM) and C (**17**, 2.6 μM); and mammeas A/AA cyclo D (**28**, 1.2 μM), B/AB cyclo D (**31**, 0.84 μM), and E/BC cyclo D (**33**, 2.3 μM) were relatively potent competitive inhibitors of human aromatase. The most potent compound, **31**, exhibited almost the same binding affinity as aminoglutethimide. Thus, coumarin constituents of *M. siamensis* may be useful agents for the treatment and prevention of estrogen-dependent breast cancer. The detailed structural requirements of coumarins leading to aromatase inhibition should be further studied.

References

1. Lake, B.G. Coumarin metabolism, toxicity and carcinogenicity: Relevance for human risk assessment. *Food Chem. Toxicol.* **1999**, *37*, 423–453. [CrossRef]
2. Bourgaud, F.; Hehn, A.; Larbat, R.; Doerper, S.; Gonitier, E.; Kellner, S.; Matern, U. Biosynthesis of coumarins in plants: A major pathway still to be unravelled for cytochrome P450 enzymes. *Phytochem. Rev.* **2006**, *5*, 293–308. [CrossRef]
3. Kostova, I. Synthetic and natural coumarins as antioxidants. *Mini-Rev. Med. Chem.* **2006**, *6*, 365–374. [CrossRef]
4. Vogt, T. Phynylpropanoid biosynthesis. *Mol. Plant* **2010**, *3*, 2–20. [CrossRef] [PubMed]
5. Venugopala, K.N.; Rashmi, V.; Odhav, B. Review on natural coumarin lead compounds for their pharmacological activity. *BioMed. Res. Int.* **2013**, *2013*, 963248. [CrossRef]
6. Musa, M.A.; Latinwo, L.M.; Virgile, C.; Badisa, V.L.D.; Gbadebo, A.J. Synthesis and in vitro evaluation of 3-(4-nitrophenyl)coumarin derivatives in tumor cell lines. *Bioorg. Chem.* **2015**, *58*, 96–103. [CrossRef] [PubMed]
7. Stefanachi, A.; Leonetti, F.; Pisani, L.; Catto, M.; Carotti, A. Coumarin: A natural, privileged and versatile scaffold for bioactive compounds. *Molecules* **2018**, *23*, 250. [CrossRef] [PubMed]
8. Srikrishana, D.; Godugu, C.; Dubey, P.K. A review on pharmacological properties of coumarins. *Mini-Rev. Med. Chem.* **2018**, *18*, 113–141. [CrossRef]
9. Pereira, T.M.; Franco, D.P.; Vitorio, F.; Kümmerle, A.E. Coumarin compounds in medicinal chemistry: Some important examples from the last years. *Curr. Top. Med. Chem.* **2018**, *18*, 124–148. [CrossRef]
10. Gançalves, G.A.; Spillere, A.R.; das Neves, G.M.; Kagami, L.P.; von Poser, G.L.; Canto, R.F.S.; Eifler-Lima, V. Natural and synthetic coumarins as antileishmanial agents: A review. *Eur. J. Med. Chem.* **2020**, *203*, 112514. [CrossRef]
11. Di Stasi, L.C. Coumarin derivatives in inflammatory bowel disease. *Molecules* **2021**, *26*, 422. [CrossRef]
12. Xu, Z.; Chen, Q.; Zhang, Y.; Liang, C. Coumarin-based derivatives with potential anti-HIV activity. *Fitoterapia* **2021**, *150*, 104863. [CrossRef]
13. Abdelmohsen, U.R.; Albohy, A.; Abdulrazik, B.S.; Bayoumi, S.A.L.; Nalak, L.G.; Khallaf, I.S.A.; Bringmann, G.; Farag, S.F. Natural coumarins as potential anti-SARS-CoV-2 agents supported by docking analysis. *RSC Adv.* **2021**, *11*, 16970. [CrossRef]
14. Morikawa, T.; Matsuda, H.; Ohgushi, T.; Nishida, N.; Ishiwada, T.; Yoshikawa, M. Absolute stereostructures of acylated khellactone-type coumarins from *Angelica furcijuga*. *Heterocycles* **2004**, *63*, 2211–2215. [CrossRef]
15. Morikawa, T.; Matsuda, H.; Nishida, N.; Ohgushi, T.; Yoshikawa, M. Structures of new aromatics glycosides from a Japanese folk medicine, the roots of *Angelica furcijuga*. *Chem. Pharm. Bull.* **2004**, *52*, 1387–1390. [CrossRef]
16. Matsuda, H.; Morikawa, T.; Ohgushi, T.; Ishiwada, T.; Nishida, N.; Yoshikawa, M. Inhibitors of nitric oxide production from the flowers of *Angelica furcijuga*: Structures of hyuganosides IV and V. *Chem. Pharm. Bull.* **2005**, *53*, 387–392. [CrossRef]
17. Yoshikawa, M.; Nishida, M.; Ninomiya, K.; Ohgushi, T.; Kubo, M.; Morikawa, T.; Matsuda, H. Inhibitory effects of coumarin and acetylene constituents from the roots of *Angelica furcijuga* on D-galactosamine/lipopolysaccharide-induced liver injury in mice and on nitric oxide production in lipopolysaccharide-activated mouse peritoneal macrophages. *Bioorg. Med. Chem.* **2006**, *14*, 456–463. [CrossRef]
18. Morikawa, T.; Sueyoshi, M.; Chaipech, S.; Matsuda, H.; Nomura, Y.; Yabe, M.; Matsumoto, T.; Ninomiya, K.; Yoshiikawa, M.; Pongpiriyadacha, Y.; et al. Suppressive effects of coumarins from *Mammea siamensis* on inducible nitric oxide synthase expression in RAW264.7 cells. *Bioorg. Med. Chem.* **2012**, *20*, 4968–4977. [CrossRef]

19. Ninomiya, K.; Shibatani, K.; Sueyoshi, M.; Chaipech, S.; Pongpiriyadacha, Y.; Hayakawa, T.; Muraoka, O.; Morikawa, T. Aromatase inhibitory activity of geranylated coumarins, mammeasins C and D, isolated from the flowers of *Mammea siamensis*. *Chem. Pharm. Bull.* **2016**, *64*, 880–885. [CrossRef]

20. Tanage, G.; Tsutsui, N.; Shibatani, K.; Marumoto, S.; Ishikawa, F.; Ninomiya, K.; Muraoka, O.; Morikawa, T. Total synthesis of the aromatase inhibitors, mammeasins C and D, from thai medicinal plant *Mammea siamensis*. *Tetrahedron* **2017**, *73*, 4481–4486. [CrossRef]

21. Morikawa, T.; Luo, F.; Manse, Y.; Sugita, H.; Saeki, S.; Chaipech, S.; Pongpiriyadacha, Y.; Muraoka, O.; Ninomiya, K. Geranylated coumarins from Thai medicinal plant *Memmea siamensis* with testosterone 5α-reductase inhibitory activity. *Front. Chem.* **2020**, *8*, 199. [CrossRef]

22. Luo, F.; Sugita, H.; Muraki, K.; Saeki, S.; Chaipech, S.; Pongpiriyadacha, Y.; Muraoka, O.; Morikawa, T. Anti-proliferative activities of coumarins from the Thai medicinal plant *Mammea siamensis* (Miq.) T. Anders. Against human digestive tract carcinoma cell lines. *Fitoterapia* **2021**, *148*, 104780. [CrossRef]

23. Mahidol, C.; Kaweetripob, W.; Prawat, H.; Ruchirawat, S. Mammea coumarins from the flowers of *Mammea siamensis*. *J. Nat. Prod.* **2002**, *65*, 757–760. [CrossRef]

24. Kaweetripob, W.; Mahidol, C.; Prawat, H.; Ruchirawat, S. Chemical investigation of *Mammea siamensis*. *Pharm. Biol.* **2000**, *38* (Suppl. 1), 55–57. [CrossRef]

25. Prachyawarakorn, V.; Mahidol, C.; Ruchirawat, S. Pyranocoumarins from the twigs of *Mammea siamensis*. *Pytochem.* **2006**, *67*, 924–928. [CrossRef]

26. Guilet, D.; Hélesbeux, J.-J.; Séraphin, D.; Sévenet, T.; Richomme, P.; Bruneton, J. Novel cytotoxic 4-phenyfuranocoumarins from *Calophyllum dispar*. *J. Nat. Prod.* **2001**, *64*, 563–568. [CrossRef]

27. Kofinas, C.; Chinou, I.; Loukis, A.; Harvala, C.; Maillard, M.; Hostettmann, K. Flavonoids and bioactive coumarins of *Tordylium apulum*. *Phytochem.* **1998**, *48*, 637–641. [CrossRef]

28. Shul'ts, E.E.; Ganbaatar, Z.; Petrova, T.N.; Shakirov, M.M.; Bagryanskaya, I.Y.; Taraskin, V.V.; Radnaeva, L.D.; Otgonsuren, D.; Pokrovskii, A.G.; Tolstikov, G.A. Plant coumarins. IX. Phenolic compounds of *Ferulopsis hystrix* growing in Mongolia, cytotoxic activity of 8,9-dihydrofurocoumarins. *Chem. Nat. Comp.* **2012**, *48*, 211–217. [CrossRef]

29. Ngo, N.T.N.; Nguyen, V.T.; Vo, H.V.; Vang, O.; Duus, F.; Ho, T.-D.H.; Pham, H.D.; Nguyen, L.-H.D. Cytotoxic coumarins from the bark of *Mammea siamensis*. *Chem. Pharm. Bull.* **2010**, *58*, 1487–1491. [CrossRef]

30. Tung, N.H.; Uto, T.; Sakamoto, A.; Hayashida, Y.; Hidaka, Y.; Morinaga, O.; Lhieochaiphant, S.; Shoyama, Y. Antiproliferative and apoptotic effects of compounds from the flower of *Mammea siamensis* 'Miq.) T. Anders. On human cancer cell lines. *Bioorg. Med. Chem.* **2013**, *23*, 158–162. [CrossRef]

31. Rungrojsakul, M.; Saiai, A.; Ampasavate, C.; Anuchapreeda, S.; Okonogi, S. Inhibitory effect of mammea E/BB from *Mammea siamensis* seed extract on Wilms' tumor 1 protein expression in a K562 leukaemic cell line. *Nat. Prod. Res.* **2016**, *30*, 443–447. [CrossRef] [PubMed]

32. Rungrojsakul, M.; Katekunlaphan, T.; Saiai, A.; Ampasavate, C.; Okonogi, S.; Sweeney, C.A.; Anuchapreeda, S. Down-regulaytory mechanism of mammea E/BB from *Mammea siamensis* seed extract on Wilm's tumor 1 expression in K562 cells. *BMC Complement. Altern. Med.* **2016**, *16*, 130. [CrossRef] [PubMed]

33. Uto, T.; Tung, N.H.; Thongjankaew, S.; Shoyama, Y. Kayeassamin A isolated from the flower of *Mammea siamensis* triggers apoptosis by activation caspase-3/-8 in HL-60 human leukemia cells. *Pharmacogn. Res.* **2016**, *8*, 244–248. [CrossRef]

34. Benson, J.R.; Ravisekar, O. Aromatase inhibitors for treatment of breast cancer. *Curr. Cancer Ther.* **2007**, *3*, 67–79. [CrossRef]

35. Monteiro, R.; Faria, A.; Azevedo, I.; Calhau, C. Modulation of breast cancer cell survival by aromatase inhibiting hop (*Humulus lupulus* L.) flavonoids. *J. Steroid Biochem. Mol. Biol.* **2007**, *105*, 124–130. [CrossRef]

36. Balunas, M.J.; Kinghorn, A.D. Natural compounds with aromatase inhibitory activity: An update. *Planta Med.* **2010**, *76*, 1087–1093. [CrossRef]

37. Shagufta, I.A. Recent development in steroidal and nonsteroidal aromatase inhibitors for the chemoprevention of estrogen-dependent breast cancer. *Eur. J. Med. Chem.* **2015**, *102*, 375–386. [CrossRef]

38. Barker, S. Non-steroidal anti-estrogens in the treatment of breast cancer. *Curr. Opin. Investig. Drugs* **2006**, *7*, 1085–1091.

39. Recanatini, M.; Cavalli, A.; Valenti, P. Nonsteroidal aromatase inhibitors: Recent advances. *Med. Res. Rev.* **2002**, *22*, 282–304. [CrossRef]

40. Sabnis, G.J.; Jevolac, D.; Lorng, B.; Brodie, A. The role of growth factor receptor pathways in human breast cancer cells adapted to long-term estrogen deprovation. *Cancer Res.* **2005**, *65*, 3903–3910. [CrossRef]

41. Santen, R.J.; Lobenhofer, E.K.; Afshari, C.A.; Bao, Y.; Song, R.X. Adaptation of estrogen-regulated genes on long-term estradiol deprived MCF-7 breast cancer cells. *Breast Cancer Res. Treat.* **2005**, *94*, 213–223. [CrossRef]

42. Khan, S.; Zhao, J.; Khan, I.A.; Walker, L.A.; Dasmahapatra, A.K. Potential utility of natural products as regulators of breast cancer-associated aromatase promoters. *Reprod. Biol. Endocrinol.* **2011**, *9*, 91. [CrossRef] [PubMed]

43. Mocanu, M.-M.; Nagy, P.; Szöllősi, J. Chemoprevention of breast cancer by dietary polyphenols. *Molecules* **2015**, *20*, 22578–22620. [CrossRef]

44. Yuan, L.; Cai, Y.; Zhang, L.; Liu, S.; Li, P.; Li, X. Promoting apoptosis, a promising way to treat breast cancer with natural products: A comprehensive review. *Front. Pharmacol.* **2022**, *12*, 801662. [CrossRef]

45. Naeem, M.; Iqbal, M.O.; Khan, H.; Ahmed, M.M.; Farooq, M.; Aadil, M.M.; Jamaludin, M.I.; Hazafa, A.; Tsai, W.-C. A review of twenty years of research on the regulation of signaling pathways by natural products in breast cancer. *Molecules* **2022**, *27*, 3412. [CrossRef] [PubMed]

46. Son, H.-U.; Yoon, E.-K.; Yoo, C.-Y.; Park, C.-H.; Bae, M.-A.; Kim, T.-H.; Lee, C.-H.; Lee, K.W.; Seo, H.; Kim, K.-J.; et al. Effects of synergistic inhibition on *α*-glucosidase by phytoalexins in soybeans. *Biomolecules* **2019**, *9*, 828. [CrossRef]

47. Kellis, J.T., Jr.; Vickery, L.E. Inhibition of estrogen synthetase (aromatase) by 4-cyclohexylanimine. *Endocrinology* **1984**, *114*, 2128–2137. [CrossRef]